AJNR

Clinical applications of proton MR spectroscopy.

M Castillo, L Kwock and S K Mukherji

AJNR Am J Neuroradiol 1996, 17 (1) 1-15
http://www.ajnr.org/content/17/1/1.citation

This information is current as
of August 14, 2025.

Special Report

Clinical Applications of Proton MR Spectroscopy

Mauricio Castillo, Lester Kwock, and Suresh K. Mukherji

Magnetic resonance (MR) spectroscopy has received little attention from the clinical radiology community. Indeed, most MR spectroscopic studies are performed by a small and dedicated group of individuals, mostly basic scientists. This behavior is partly because MR spectroscopy does not produce "pictures" but results in "graphs," and until lately, it could only be obtained with dedicated units and software. At present, MR spectroscopy may be obtained with many clinical 1.5-T MR units and commercially available software. Adequate MR spectra may be obtained in periods of time as short as 10 to 15 minutes. Therefore, they may be added to routine MR imaging studies without significant time penalties. Moreover, MR spectroscopy provides greater information concerning tissue characterization than what is possible with MR imaging studies alone. This article will review the current status of proton MR spectroscopy with emphasis on its clinical utility for evaluation of neurologic disorders. Also, we include a section on some innovative and promising uses of proton MR spectroscopy. The information provided here is simplified in the hope that its understanding will lead to increased use of proton MR spectroscopy by clinical radiologists.

History

Purcell et al (1) and Bloch et al (2) elucidated the principles of nuclear magnetic resonance in 1946. Five years later, Proctor and Yu (3) proposed that the resonance frequency of a nucleus depends on its chemical environment, which produces a small, but perceptible, change in the Larmor resonance frequency of that nucleus. This nuclear behavior is termed "chemical shift," and is caused by the magnetic fields generated by circulating electrons surrounding the nuclei interacting with the main magnetic field. Protons (^{1}H) have been traditionally used for MR spectroscopy because of their high natural abundance in organic structures and high nuclear magnetic sensitivity compared with any other magnetic nuclei (4). Moreover, diagnostically resolvable hydrogen MR spectra may be obtained with clinical instruments (1.5 T or greater) and routine surface coils. Phosphorus 31 MR spectroscopy has also been used clinically to study changes in high energy metabolism in a number of pathologic processes. However, because of the scope of this report, phosphorus 31, carbon 13, sodium 23, and fluorine 19 MR spectroscopy will not be addressed here.

Technique

After the nuclei have been exposed to a uniform magnetic field, they receive a 90° radio frequency pulse that rotates them from the z-axis to the x-axis. When this pulse is turned off, the nuclei return to their original position in the z-axis. The time it takes them to return to their original position in the z-axis is governed by their relaxation times. The receiving coil detects the voltage variations at many points in time during this period. This voltage variation is termed *free induction decay* and may be plotted as an exponential decay function (ie, intensity versus time) to yield time domain information (ie, relaxation times). Fourier transformation of this information yields information in the frequency domain, namely, a plot of peaks at different Larmor frequencies. The parameters that characterize each peak include its resonance frequency, its height, and its width at half-height (4). The resonance frequency position of each peak on the plot is dependent on the chemical environment of that nucleus and is usually expressed as parts per million from the main

From the Department of Radiology, University of North Carolina School of Medicine, Chapel Hill.

Address reprint requests to Mauricio Castillo, Radiology, CB 7510, 3324 Old Infirmary, University of North Carolina at Chapel Hill, Chapel Hill, NC 27599-7510.

Index terms: Brain, magnetic resonance; Magnetic resonance, spectroscopy; Magnetic resonance, tissue characterization; Special reports

AJNR 17:1–15, Jan 1996 0195-6108/96/1701–0001 © American Society of Neuroradiology

magnetic resonance frequency of the system used (ie, chemical shift). The height (maximum peak intensity) or the area under the peak may be calculated and yield relative measurements of the concentration of protons. The resonance frequency/chemical shift position gives information regarding the chemical environment of protons. The width of the peak at half-height gives relaxation time information because it is proportional to 1/T2.

Artifacts introduced by magnetic field inhomogeneities may result in distortion of the line width of the peaks and decreased ability to resolve them. Therefore, a homogenous magnetic field is an important prerequisite to obtaining "resolvable" spectra. Shimming the field in the region of interest to the resonance of water assures the homogeneity of the field. The water line width should be less than 0.2 ppm after shimming. Spatial localization is achieved by applying static and/or pulsed gradients. Localization methods commonly used in a clinical proton MR spectroscopy include: depth-resolved surface coil spectroscopy (DRESS), point-resolved surface coil spectroscopy (PRESS), spatially resolved spectroscopy (SPARS), and the stimulated-echo method (STEAM) (5–7). At our institution, we use PRESS and STEAM. For practical purposes, STEAM allows for shorter echo times, thereby improving resolution of the metabolites; however, it is more sensitive to motion, whereas the PRESS technique is less sensitive to motion. Because the signal from the water peak is very large when compared with that of other metabolites, it needs to be suppressed for adequate visualization of other peaks (the concentration of water can be 10 000 times the concentration of other metabolites). The most frequently used method for suppressing the signal from water is chemical shift selective excitation (CHESS), which reduces the water signal by a factor of 1000.

The term *voxel* refers to the volume element that is being sampled. This volume element has a width, length, and depth. In clinical spectroscopy, the size of the voxel generally varies between 2 and 8 cm^3, but with current equipment, it may be as small as 1 cm^3. Smaller voxels contain smaller amounts of tissues and produce lesser signal-to-noise ratios. Therefore, the number of signal averages required to obtain good signal to noise needs to be increased with smaller voxels. With voxels of 8 cm^3, approximately 100 signal averages are required to obtain adequate spectra. At present, most of our MR spectroscopic studies are obtained using a localized single volume (Fig 1). However, using chemical-shift imaging it is possible to obtain one- or two-dimensional data sets that display metabolites from adjacent compartments encompassing a large tissue volume (Fig 2). Two-dimensional chemical-shift proton MR spectroscopy allows the mapping of metabolite concentrations to be manipulated by computer and superimposed on the image of an abnormality illustrating the distribution of such metabolites within that area (8). Different colors may be assigned to each metabolite to facilitate visual understanding of their distribution. Although most modern clinical MR spectroscopy units are capable of echo times (TEs) as short as 20 milliseconds, adequate MR spectra may be obtained with TEs as long as 136 to 272 milliseconds. Using long TEs, the signal from most metabolites in the brain is lost except that of choline (Cho), creatine (Cr), *N*-acetyl aspartate (NAA), and lactate. Conversely, short TEs allow for identification of many other metabolites (eg, myoinositol, glutamate, glutamine, and glycine). MR spectra may be obtained during a 10- to 15-minute session. Therefore, MR spectroscopy may be incorporated as part of a

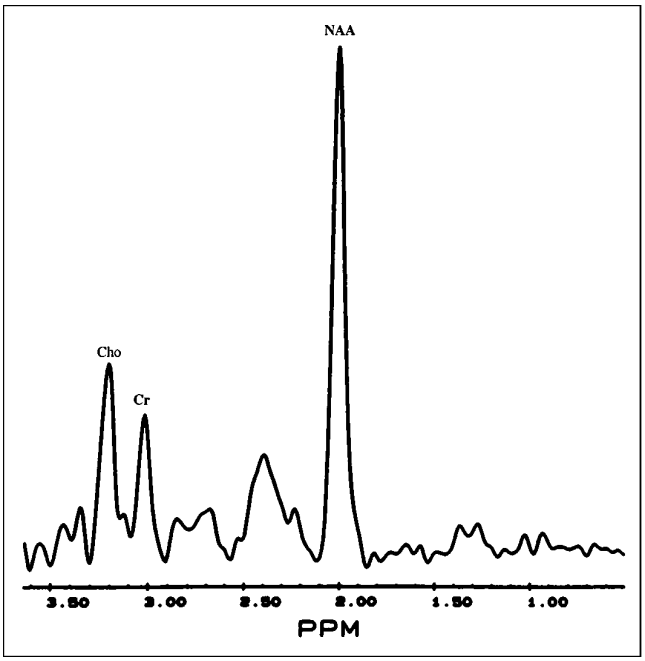

Fig 1. Normal brain proton MR spectroscopy, single voxel. Proton MR spectroscopy obtained in a healthy volunteer using a single 8-cm^3 volume element in right centrum semiovale.

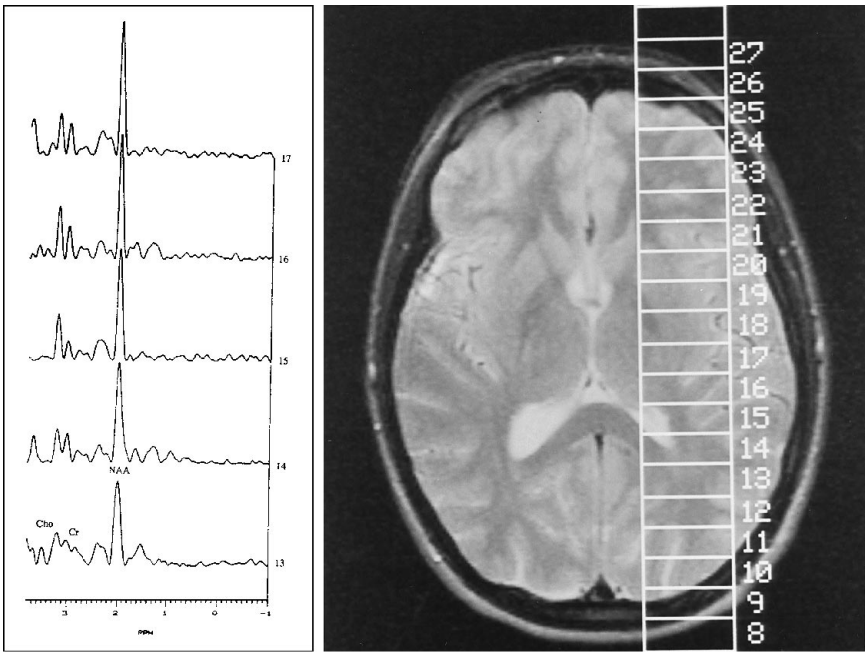

Fig 2. Normal brain proton MR spectroscopy, one-dimensional chemical-shift image.

A, Normal spectra obtained from adjacent brain volumes (volumes 13 to 17). The concentration of NAA relatively increases in regions that contain larger areas of gray matter—in this case, the basal ganglia.

B, Corresponding MR T2-weighted image (4000/93/1 [repetition time/TE/excitations]) demonstrates location of volumes. MR spectroscopy is shown only for volumes 13 to 17.

routine imaging study without a significant time penalty. At our institution, we have created a set of "shim files," which allows the technologist to perform the study easily by setting the location of the voxel and tailoring its size to correspond grossly to the abnormality in question. A voxel should include as much of the abnormality as possible and little (generally less than 20% of the voxel size) normal surrounding brain.

Metabolites, Location, and Significance

There is evidence that the concentration of normal metabolites in the brain varies according to the patient's age (9) (Fig 3). This variation is more noticeable during the first 3 years of life but may be seen up to 16 years of age. The most striking variation is an increase in NAA/Cr ratio and a decrease in the Cho/Cr ratio as the brain matures. These changes may reflect neuronal maturation and an increase in the number of axons, dendrites, and synapses. It is unclear whether any significant changes are observed with advancing age.

NAA

The presence of NAA is attributable to its *N*-acetyl methyl group, which resonates at 2.0 ppm (Fig 1). This peak also contains contributions from less-important *N*-acetyl groups. NAA is accepted as a neuronal marker, and as such, its concentration will decrease with many insults to the brain (10). The exact role of NAA in the brain is not known. Glutamate and *N*-acetyl-aspartyl-glutamate are colocalized with NAA in neurons. Breakdown of *N*-acetyl-aspartyl-glutamate releases both NAA and glutamate, and subsequent breakdown of NAA leads to aspartate. These compounds are excitatory amino acids and are increased with ischemia. It is possible that, in the near future, concentrations of *N*-acetyl-aspartyl-glutamate and glutamate may serve to monitor treatments designed to protect brain tissues by blocking excitatory amino acids. NAA is not present in tumors outside the central nervous system. Canavan disease is the only disease in which NAA is increased. In normal spectra, NAA is the largest peak.

Cho

The peak for Cho occurs at 3.2 ppm (Fig 1). It contains contributions from glycerophosphocholine, phosphocholine, and phosphatidylcholine and therefore reflects total brain choline stores. Cho is a constituent of the phospholipid metabolism of cell membranes and reflects membrane turnover, and it is a precursor for acetylcholine and phosphatidylcholine (10). The latter compound is used to

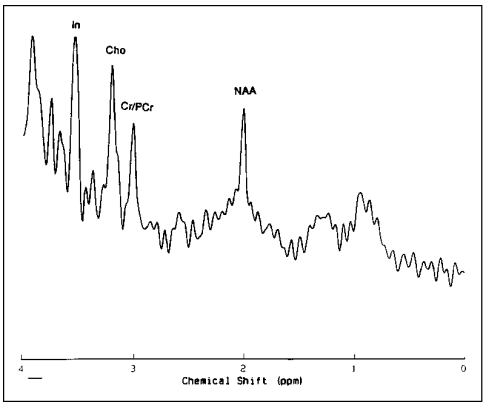

Fig 3. Normal newborn brain. Single-voxel proton MR spectroscopy in a healthy newborn shows relatively smaller concentration of NAA with respect to Cho and Cr. This probably reflects neuronal immaturity. Inositol (*In*) is prominent and normal at this age.

build cell membranes, whereas the former is a critical neurotransmitter involved in memory, cognition, and mood. Therefore, increased Cho probably reflects increased membrane synthesis and/or an increased number of cells.

Cr

The peak for Cr is seen at 3.03 ppm and contains contributions from Cr, Cr phosphate, and, to a lesser degree, γ-aminobutyric acid, lysine, and glutathione (Fig 1). An additional peak for Cr may be visible at 3.94 ppm. Therefore, the Cr peak is sometimes referred to as "total Cr." Cr probably plays a role in maintaining energy-dependent systems in brain cells by serving as a reserve for high-energy phosphates and as a buffer in adenosine triphosphate and adenosine diphosphate reservoirs (11). Cr is increased in hypometabolic states and decreased in hypermetabolic states. In normal spectra, Cr is located to the immediate right of Cho and is the third-highest peak. Because this peak remains fairly stable even in face of disease, it may be used as a control value.

Lactate

The lactate peak has a particular configuration. It consists of two distinct, resonant peaks called a "doublet" and is caused by the magnetic field interactions between adjacent protons (J coupling). This lactate doublet occurs at 1.32 ppm. A second peak for lactate occurs at 4.1 ppm. Because this latter peak is very close to the water, it is generally suppressed. Normally, lactate levels in the brain are low. The presence of lactate generally indicates that the normal cellular oxidative respiration mechanism is no longer in effect, and that carbohydrate catabolism is taking place (12). Lactate can play a role as a neuromodulator by altering the excitability of local neurons (12). Confirmation that a peak at 1.32 ppm corresponds to lactate may be done by altering the TE. At a TE of 272 milliseconds, lactate projects above the baseline, whereas at a TE of 136 milliseconds, the lactate doublet is inverted below the baseline.

Myoinositol

Myoinositol is a metabolite involved in hormone-sensitive neuroreception and is a possible precursor of glucuronic acid, which detoxifies xenobiotics by conjugation (13). The myoinositol peak occurs at 3.56 ppm. Decreased myoinositol content in the brain has been associated with the protective action of lithium in mania and the development of diabetic neuropathy (14). In addition, a triphosphorylated derivative of myoinositol, myoinositol-1,4,5-triphosphate, is believed to act as a second messenger of intracellular calcium-mobilizing hormones (14). The combination of elevated myoinositol and decreased NAA may be seen in patients with Alzheimer disease (15). The myoinositol peak is significant in tissues outside the central nervous system, for example, in head and neck carcinomas.

Glutamate and Glutamine

Glutamate is an excitatory neurotransmitter, which plays a role in mitochondrial metabolism (13). Gamma-amino butyric acid is an important product of glutamate. Glutamine plays a role in detoxification and regulation of neurotransmitter activities (16). These two metabolites resonate closely together and they are commonly represented by their sum as peaks located between 2.1 and 2.5 ppm.

Alanine

Alanine is a nonessential amino acid whose function is uncertain. Its peak occurs between

1.3 and 1.4 ppm and therefore may be overshadowed by the presence of lactate. Alanine, similar to lactate, inverts when the TE is changed from 136 to 272 milliseconds.

Lipids

Membrane lipids in the brain have very short relaxation times and are normally not observed unless very short TEs are used. The protons of lipids produce peaks at 0.8, 1.2, 1.5, and 6.0 ppm. These peaks comprise methyl, methylene, allelic, and the vinyl protons of unsaturated fatty acids (17). These metabolites may be increased in high-grade astrocytomas and meningiomas and may reflect necrotic processes (16). However, it is also important to remember that normal lipid resonances arising from fat may be the result of voxel contamination by fat located in the subcutaneous scalp; they are normally much less intense or absent at a TE of 272 milliseconds because of their short relaxation times.

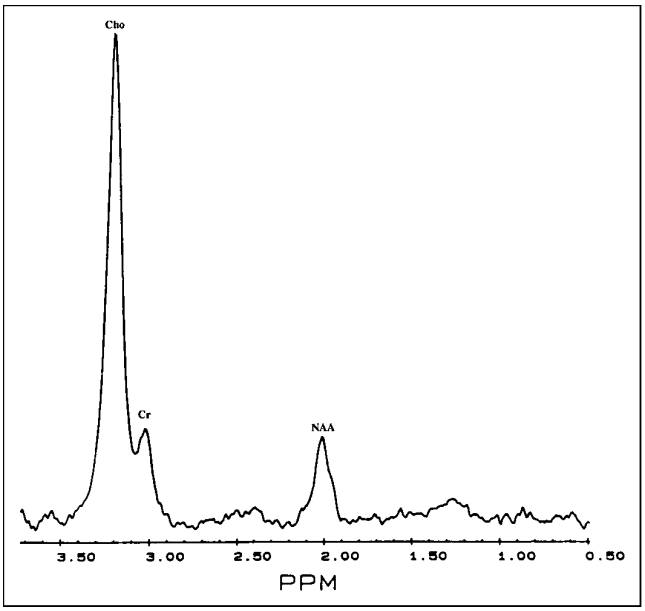

Fig 4. Glioblastoma multiforme. Single 8-cm^3 voxel from surgically proved glioblastoma multiforme shows low NAA and markedly elevated Cho. Although lactate may be present in high-grade astrocytomas, it is not seen in this tumor.

Clinical Applications

Astrocytomas

Proton MR spectroscopy readily distinguishes normal brain tissues from astrocytomas (18–20). However, proton MR spectroscopy may not be able to distinguish between different histologic grades of malignancy in astrocytomas (21). Some investigators have proposed that the presence of lactate correlates with a higher degree of malignancy and that it is commonly observed in glioblastoma multiforme (8, 22). The typical proton MR spectroscopic characteristics of astrocytomas include a significant reduction in NAA, a moderate reduction in Cr, and an elevation of Cho (19) (Fig 4). Reduction of NAA probably indicates a loss of normal neuronal elements as they are destroyed and/or substituted by malignant cells. In astrocytomas, the NAA is reduced to 40% to 70% of that in normal brain (10). Reduction of Cr is probably related to an altered metabolism, and elevation of Cho may reflect increased membrane synthesis and cellularity (both of which are present in tumors) (8). Elevation of lactate may reflect tumor hypoxia. The Cho peak also is increased in the more-malignant astrocytomas (10). Proton MR spectroscopy may be used to distinguish infection from a tumor, because the former has extremely low concentrations of Cho (10).

Proton MR spectroscopy may also play a role in monitoring the response of astrocytomas to treatment (8). In some instances, proton MR spectroscopy may detect tumor recurrence before MR images become abnormal.

Meningiomas

Although the diagnosis of a meningioma is usually straightforward from the MR images, proton MR spectroscopy may be useful in difficult cases. Because meningiomas arise outside the central nervous system, theoretically they do not contain NAA (19). The signal of Cho is, however, markedly increased (up 300 times normal) particularly in recurrent meningiomas (21). Lactate and alanine may be also elevated in some meningiomas (19). There is no clear explanation for the increase in alanine in meningiomas. The above proton MR spectroscopic features are seen in typical meningiomas (fibrous type). Atypical and malignant meningiomas, or those that invade the brain, may show resonances in the location of NAA, and differentiating them from astrocytomas may prove difficult. Unfortunately, in our experience, meningiomas generally show MR spectra that are indistinguish-

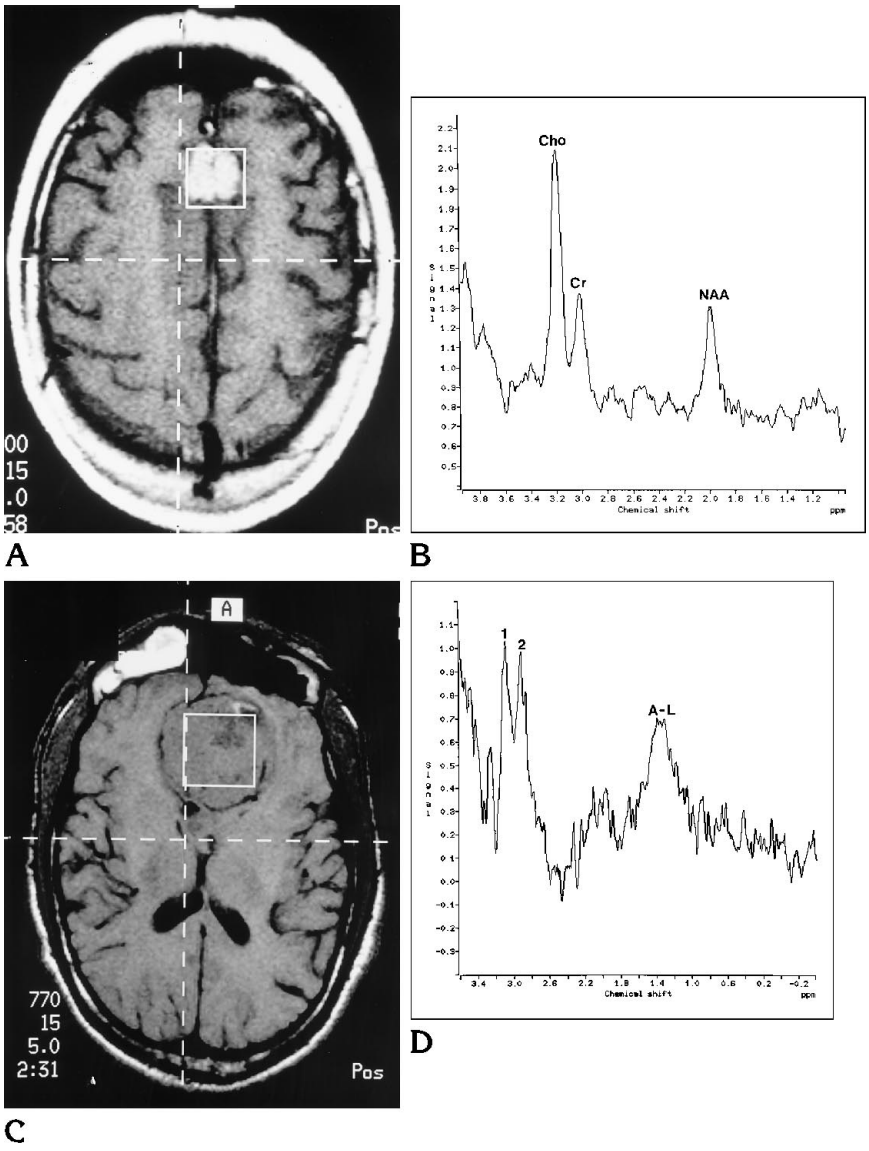

Fig 5. Meningioma.

A, Axial postcontrast MR T1-weighted image (600/15/1) shows the position of a single voxel, which tightly fits the lesion with little contribution from the surrounding brain.

B, Proton MR spectroscopy shows patterns similar to those seen in astrocytomas with elevated Cho and low NAA. There is no obvious lactate or alanine. Spectra were obtained before contrast was given.

C, Axial precontrast MR T1-weighted image (770/15/1) shows location of the volume of interest within a frontobasal meningioma (surgically proved).

D, Proton MR spectra show Cho (*1*), Cr (*2*), and a peak (*A–L*) at 1.3 to 1.4 ppm, corresponding to alanine and/or lactate. No definite NAA is identified.

able from those of astrocytomas and only rarely show the alanine peak (Fig 5). The presence of NAA may be related to a partial volume-averaging artifact from adjacent brain included in the volume of interest. Other extraaxial masses, such as schwannomas, also show increased lipid, lactate, and Cho peaks.

Metastases

In adults with multiple brain lesions the primary differential diagnosis is that of metastases. In the presence of a single lesion, differentiating between primary and secondary brain tumors is important but not often possible. Unfortunately, proton MR spectroscopic findings are also nonspecific in this situation (21, 23). Metastases commonly show moderate to marked reduction of NAA, a decreased Cr signal, and elevated Cho (Fig 6). Obviously, these features are identical to those present in astrocytomas (see above). Some metastases (particularly those from breast carcinomas) may also contain lipids (24). Lipid resonance may also be present in high-grade astrocytomas and is caused by the presence of necrosis. Metastases to the brain pose challenging demands to the spectroscopist, because their small size may require small voxels and a larger number of signal averages. If analyzed with larger voxels, which may include normal surrounding tissues, par-

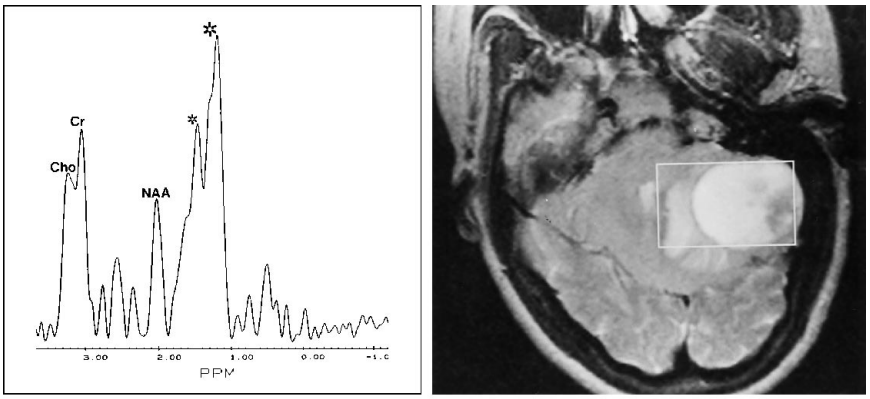

Fig 6. Metastasis.

A, Single-volume proton MR spectroscopy in a solitary brain metastasis (proved small-cell carcinoma). Note decreased NAA with respect to Cho and Cr, which appear elevated. Large peaks (*small* and *large asterisks*) are probably combination of lactate and lipids.

B, Axial MR T2-weighted image (4000/93/1) shows the position of the voxel with respect to the lesion. Note that the voxel is eccentric to the lesion to avoid skull and subcutaneous fat. The tumor occupies approximately 80% of the voxel.

tial volume artifacts that render the MR spectra suboptimal may result. In addition, because of the peripheral location of these lesions, lipids from the subcutaneous scalp fat may contaminate the sample.

Radiation injury

Histologically, radiation injury is characterized by damage to the vascular endothelium that may result in ischemia and necrosis. Proton MR spectroscopy shows elevation of lactate in patients who have received 40 Gy or more to the brain (25). This abnormality is appreciable even when the MR imaging studies are normal. Therefore, proton MR spectroscopy may be promising as a tool for the detection of radiation injury before it becomes evident by MR imaging.

Radiation necrosis may be indistinguishable from residual and recurrent tumors by computed tomography, MR, single-photon emission computed tomography, and even positron emission tomographic imaging (25). At our institution, 25 patients with brain tumors treated with a combination of radiation and chemotherapy underwent serial proton MR spectroscopic studies (Ende J, Scatliff JH, Powers S, et al, "Spectral proton and P-31 MR Spectroscopy Patterns of Treated Human Brain Tumors," presented at the 11th Annual Meeting of the Society of Magnetic Resonance in Medicine, Berlin, Germany 1992). In 9 patients with tumor recurrence, proton MR spectroscopy showed elevated Cho/NAA, Cho/Cr, and the presence of lactate (Fig 7A and B). Eight patients with radiation necrosis showed highly depressed levels of NAA, Cho, and Cr and an intense and broad peak between 0 and 2.0 ppm. This peak is consistent with tissue necrosis. This cellular breakdown peak probably consists of free fatty acids, lactate, and amino acids (Fig 7C). Elevated lactate, reflecting severe tissue ischemia and/or mitochondrial damage, was also present in these patients.

Human Immunodeficiency Virus (HIV) Infection

In more than 60% of persons with acquired immunodeficiency syndrome (AIDS), a dementia complex will develop (26). MR imaging findings, which include diffuse brain atrophy and white matter hyperintensities in the frontoparietal regions on T2-weighted images, are evident only in advanced cases. Therefore, it would be advantageous to develop a method that may detect the AIDS dementia complex before it becomes evident by physical examination or by MR imaging. Proton MR spectroscopy demonstrates marked metabolic alterations in patients with only mild AIDS-related dementia. The metabolic abnormalities increase proportionally with the severity of the diseases (27). Also, MR spectral abnormalities correlate with diffuse, but not with focal, signal abnormalities on MR imaging studies (28). In patients with AIDS dementia complex, proton MR spectroscopy shows a net reduction of NAA and decreases of NAA/Cho and NAA/Cr ratios (Fig 8). In patients with very low CD4 lymphocyte counts and abnormal MR imaging studies of the brain, the Cho/Cr ratio is increased (inferring a net increase in Cho) (26).

HIV-infected mothers may transmit the virus to their offspring. Approximately 25% to 40% of these newborns will seroconvert eventually

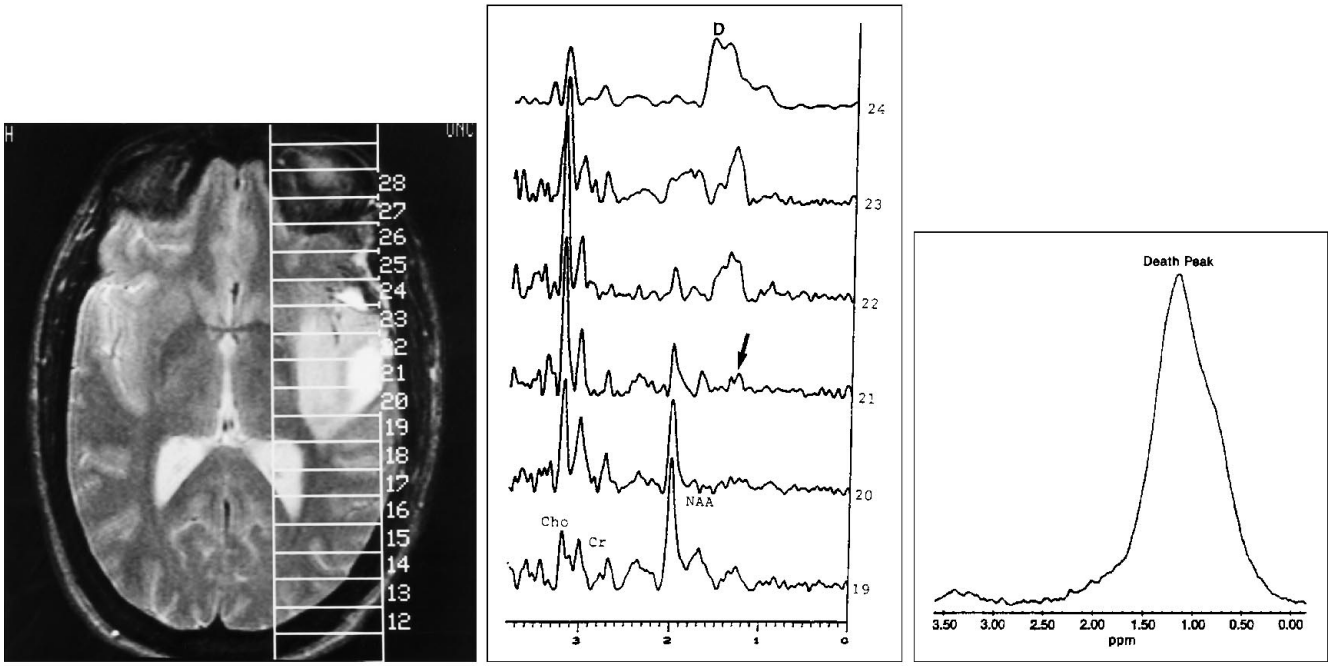

Fig 7. Recurrent tumor versus radiation necrosis.

A, Axial MR T2-weighted image (2300/90/1) in a patient after resection of a left temporal anaplastic astrocytoma and treatment with intraarterial chemotherapy and radiation. There is an abnormal area of increased signal intensity encompassed in volumes 19 to 24. No enhancement was present after gadolinium administration.

B, Proton MR spectroscopy in volumes 19 to 24. The concentrations of Cho, Cr, and NAA are normal in volume 19. Volume 21 shows low NAA, high Cho, and lactate (*arrow*) compatible with a recurrent tumor (later proved by surgery). Volume 24 shows no NAA, low Cho, and a "death peak" (*D*) (combination of lactate and cellular breakdown products). At surgery, this region was necrotic brain probably as a sequela of irradiation.

C, Single-voxel proton MR spectroscopy in a surgically proved region of radiation-induced necrosis shows large death peak.

(29). Determining positive seroconversion during the initial 6 months of life may be difficult. Despite normal MR brain images, HIV-positive newborns may show abnormal proton MR spectra as early as 10 days after birth (29). These abnormalities include higher NAA/Cr and Cho/Cr ratios than in healthy control subjects. Also, in these patients abnormal resonances between 2.1 and 2.6 ppm (overlapping the NAA peak) may be present. These have been termed "marker peaks," and their significance is not known.

Degenerative Disorders of the Elderly: Alzheimer and Parkinson Diseases

Alzheimer disease is a common disorder accounting for more than 40% of dementias in the elderly (30). Histologically, it is characterized by neuronal loss, neurofibrillary tangles, and amyloid deposits. However, because these changes also occur with normal aging, they need to be extensive before the diagnosis of Alzheimer disease may be made with certainty. Biochemically, Alzheimer disease is characterized by decreased cortical acetylcholine caused by a loss of cholinergic cells that are critical for normal memory and cognition. The clinical manifestations of the disease may be subtle and insidious, and often the diagnosis is difficult. A noninvasive tool with which to diagnose early Alzheimer disease is therefore highly desirable. Two clinical series with a total of 76 patients with Alzheimer disease in which proton MR spectroscopy was used to study the brain have been published in the radiology literature (30, 31). In both studies, NAA was decreased, and myoinositol was increased. These findings were present even in cases of mild to moderate dementia. Recently, it has been suggested that the decrease in NAA may be caused by acute deafferentation in the brains of patients with

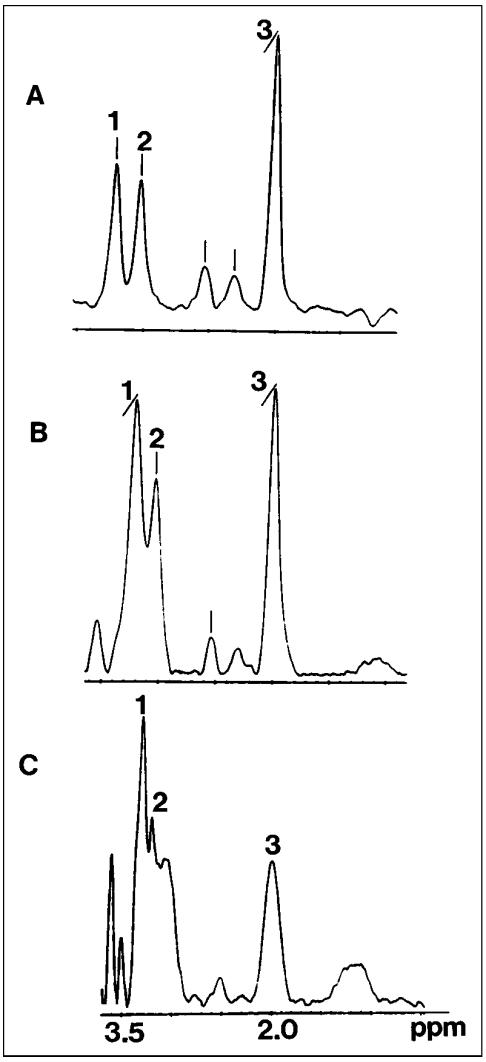

Fig 8. HIV infection.

A, Single-voxel proton MR spectroscopy in a high-risk patient (intravenous drug user and homosexual) who is HIV negative at this time. (For all figures, *1* indicates Cho; *2*, Cr; and *3*, NAA.)

B, Single voxel (same location as *A*) in same patient after seroconverting to HIV positive. The NAA has decreased relative to Cho and Cr.

C, Single voxel (same location as *A* and *B*) in same patient at the time of severe dementia and 2 weeks before death. Note the marked decrease in NAA probably related to neuronal loss or dysfunction.

Alzheimer disease, which is reflected by a transsynaptic decrease in NAA levels (32). Therefore, proton MR spectroscopy shows promise as an early diagnostic tool for Alzheimer disease. It remains to be determined whether Cho (reflecting the presence of acetylcholine) is decreased in patients with Alzheimer disease. Other dementias do not commonly show alterations of myoinositol (30).

Parkinson disease is characterized by reduced activity of the electron transport chain in the substantia nigra, platelets, and muscle (33). These findings imply that Parkinson disease is a systemic disease in which there is a dysfunction of the mitochondrial electron transport chain. In these patients, NAA, Cho, and Cr are normal, but lactate is increased (33). Patients with superimposed dementia have a more significant elevation of lactate than do patients with isolated Parkinson disease.

Degenerative Disorders in Children

The clinical symptoms and imaging features of degenerative brain disorders presenting during childhood tend to be nonspecific. Although many of these disorders have specific biochemical markers, a noninvasive method that provides an early diagnosis and could be used to follow up these children is desirable. Demyelinating childhood disorders show low NAA/Cr ratios (34). The lowest ratios are found in children with severe atrophy and white matter changes. Similar proton MR spectroscopic findings are also present in children with neuronal degenerative disorders. Patients with Alexander, Schilder, Cockayne, Leigh, and Pelizaeus-Merzbacher diseases also show decreased NAA and elevated lactate (35). Unfortunately, these abnormalities are nonspecific and do not permit differentiation of these disorders. Patients with childhood adrenoleukodystrophy show, by proton MR spectroscopy, decreased NAA/Cr and increased Cho/Cr ratios (36). These patients also show elevations of the lactate, glutamate, glutamine, and inositol peaks. The only disorder in which proton MR spectroscopy may provide a conclusive diagnosis is Canavan disease (37, 38). These children show a marked increase of the NAA peak (Fig 9). Biochemically, this occurs because of a deficiency in the enzyme aspartoacyclase, whose function is to break down NAA. When this enzyme does not function properly, NAA increases. Elevated concentration of NAA may be at least partly responsible for the degeneration of the brain present in these patients.

MELAS is a rare disorder clinically characterized by *m*itochondrial myopathy, *e*ncephalopathy, *l*actic *a*cidosis, and *s*trokes (39). Although many children with this disorder have abnormal MR imaging findings (abnormal signal intensity in the basal ganglia and infarctions) that in the

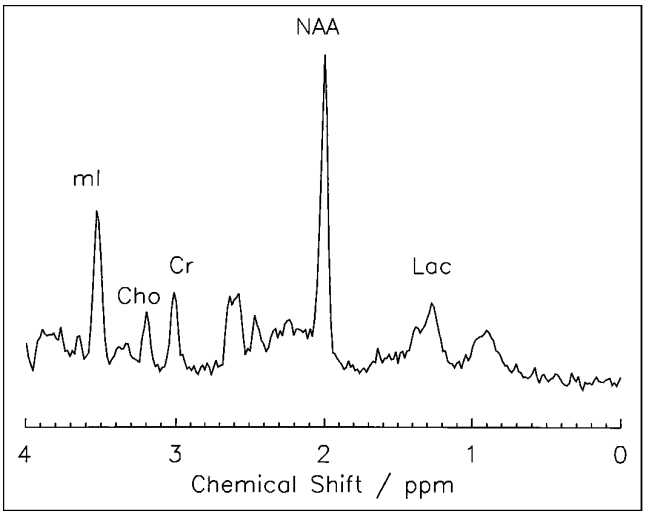

Fig 9. Canavan disease. Single-voxel proton MR spectroscopy in a patient with Canavan disease shows marked elevation of NAA. *Lac* indicates lactate. (Courtesy of Drs R. A. Zimmerman and Z. Wang, Childrens Hospital of Philadelphia.)

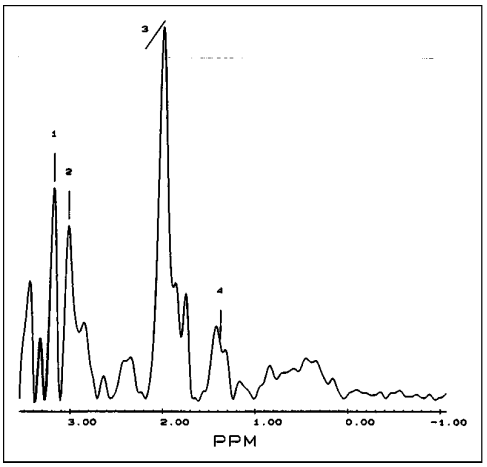

Fig 10. MELAS syndrome. Single-voxel proton MR spectroscopy over the centrum semiovale in a patient with MELAS syndrome shows normal Cho (*1*), Cr (*2*), and NAA (*3*) and mild elevation of lactate (*4*) (from Castillo et al [39]).

correct clinical setting may suggest the disorder, MELAS is a group of disorders with variable clinical expression, and in some patients, MR imaging of the brain may be normal or near-normal. In patients with this disorder, proton MR spectroscopy shows an elevation of lactate (39, 40) (Fig 10). Lactate normalizes in chronic infarctions, which also show a decrease in NAA.

Hepatic Encephalopathy

This type of encephalopathy results from cirrhosis and other chronic liver disorders. It is clinically characterized by changes in mood and behavior, tremors, dysarthria, dementia, and myelopathy (41). Establishing the diagnosis of hepatic encephalopathy with certainty in many patients is difficult; moreover, many patients have a subclinical form of the disease. In patients with hepatic encephalopathy, proton MR spectroscopy shows an elevation of glutamine levels and a reduction in Cho and myoinositol levels (42). Indeed, a reduction in the levels of myoinositol is even present in patients with liver disease but who have no overt neurologic impairment (41, 42). Therefore, it may be possible to screen for subclinical hepatic encephalopathy with proton MR spectroscopy.

Cerebral Ischemia

Because early and aggressive treatment (including intraarterial thrombolysis performed by radiologists) of cerebral infarctions is being currently evaluated, a noninvasive diagnostic test that confirms the presence of hyperacute strokes is desirable. Computed tomography changes are difficult to identify during the first 24 hours after the ictus. Although MR imaging abnormalities may be present as early as 3 hours after the onset of symptoms, permanent tissue damage may be already present at that time. In humans, proton MR spectroscopy performed in the initial 24 hours after a stroke shows elevation of lactate implying ischemia (43) (Fig 11). Decreased NAA may be observed as early as 4 days after infarction (44). Chronic infarctions show decreased NAA, Cr, and Cho, but no evidence of lactate (45). Experimentally, an increase in lactate may be detected after only 2 to 3 minutes of cerebral ischemia (46). In these animals, the lactate returned to normal when the hypoxic insult was reversed. The role of proton MR spectroscopy in the evaluation of human hyperacute cerebral infarction still needs to be evaluated.

White matter hyperintensities on T2-weighted MR images are common and are found in approximately 30% of patients older than 60 years of age (47). Their cause is uncertain but differentiating them from true infarctions is important. Proton MR spectroscopy shows that these age-related white matter changes contain normal levels of NAA and Cr (48). Their Cho level is increased, suggesting an alteration of the white matter phospholipids. They do not contain lactate.

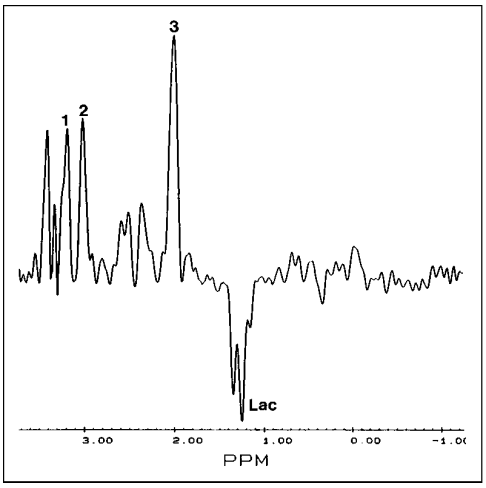

Fig 11. Acute ischemia. Single-volume proton MR spectroscopy in the right temporal region in a patient with a suspected middle cerebral artery infarct. MR spectroscopy obtained within 48 hours of ictus shows normal concentrations of Cho (*1*), Cr (*2*), and NAA (*3*). Note that in this study obtained with a TE of 136 milliseconds, the lactate doublet (*Lac*) is inverted. NAA is normal, because neuronal loss does not occur this early.

Systemic disorders, which result in central nervous system vasculitis, may be subclinical for prolonged periods of time. Patients with lupus erythematosus have decreased NAA/Cr ratios (49). These ratios are lower in patients with concomitant severe cerebral atrophy and probably reflect neuronal loss.

Seizure Foci: Hippocampal Sclerosis and Rasmussen Encephalitis

Hippocampal sclerosis may be pathologically identified in approximately 65% of patients with temporal lobe seizures (50). MR imaging can identify hippocampal abnormalities in 70% of these patients. Visual determination of hippocampal abnormalities is also difficult, particularly in patients with bilateral involvement. Having a noninvasive tool that could lateralize the focus of seizures in all patients would be desirable. Proton MR spectroscopy of the hippocampus is difficult to obtain because of its small size (which requires the use of very small voxels) and because of the presence of adjacent bone in the floor of the middle cranial fossa that introduces magnetic susceptibility artifacts. By proton MR spectroscopy, the epileptogenic hippocampus shows decreased NAA/Cho ratios, an increased or a normal Cho/Cr ratio, and occasionally elevated lactate (51). The reduction in NAA corresponds with the neuronal loss seen on histology. Because these abnormalities are not present in the normal hippocampus, abnormal proton MR spectra seem to be excellent markers for locating a seizure focus. It has been recently shown that shortly after the onset of status epilepticus, the hippocampi may become swollen (Tien RD, Felsberg GJ, "The Genesis of Human Mesial Temporal Sclerosis after Status Epilepticus: Evaluation with Sequential High-Resolution Fast Spin-Echo MR Imaging, presented at 33rd Annual Meeting of the American Society of Neuroradiology, Chicago, 1995). This abnormality may resolve on follow-up MR imaging studies or result in hippocampal sclerosis. Proton MR spectroscopy of the acutely swollen hippocampus showed normal concentrations of NAA, Cho, and Cr, but increased lactate, suggesting that ischemia may precede and predispose to hippocampal sclerosis.

Rassmussen encephalitis is a devastating cause of unilateral epilepsy (epilepsia partialis continua). As many as half of these patients have histories of infectious diseases before the onset of seizures (52). This disorder has been associated with infection by the Epstein-Barr virus and cytomegalovirus. Pathologically, there are atrophy and chronic inflammatory changes in the involved region. MR imaging shows volume loss and areas of increased T2 signal intensity, generally confined to one cerebral hemisphere. In our experience, there is severe loss of NAA in the affected region by proton MR spectroscopy. More importantly, we have observed decreased NAA in contralateral cerebral hemispheres, which were normal on MR imaging. Because functional hemispherectomy may be indicated for the control of pharmacologically refractory seizures in these patients, knowledge that abnormalities are present in both hemispheres may preclude this type of treatment.

Some Innovative Applications of MR Spectroscopy

Measurement of Psychoactive Drugs

The best-known application of proton MR spectroscopy for the measurement of psychoactive drugs in humans is the quantification of brain lithium (53). Lithium is a drug used for the treatment of patients with bipolar disorders and probably acts by decreasing the transport of Cho into cells (10). Measurements of serum

lithium levels do not have a clear relationship to recurrence of this disorder. Approximately 30% to 50% of patients with therapeutic serum levels of lithium will experience a relapse each year (53). Gonzalez et al (54) have developed a method using proton MR spectroscopy that provides adequate measurement of brain lithium in humans. This highly reliable method may play an important future role in the treatment of bipolar disorders. It remains to be determined whether proton MR spectroscopy will show a reduction in brain Cho levels in patients receiving lithium therapy.

Neurofibromatosis Type 1

By MR imaging, approximately 43% of patients with neurofibromatosis type 1 will show areas of increased T2 signal intensity in the brain (55). These lesions tend to remain static over time or to decrease in size. They are not malignant, and for lack of a better term they are called "hamartomas." In this group of patients, 6% to 15% will develop cerebral astrocytomas. These are commonly of low histologic grade and may be indistinguishable from the so-called hamartomas by MR imaging alone. We have successfully used proton MR spectroscopy to characterize these hamartomas (56). In our series, 10 patients with neurofibromatosis type 1 and cerebral lesions, which were presumed to represent hamartomas (unchanged in size during a 3-year period, no mass effect or edema, and no contrast enhancement), were examined with localized MR spectroscopy volumes. When the results obtained from the lesions were then compared with those obtained from the brains of healthy volunteers, no significant differences were found (Fig 12). This observation implies that lesions in patients with neurofibromatosis type 1 may be assumed to be benign when their proton MR spectra are that of (or very close to) normal brain. Because astrocytomas have significantly different proton MR spectra than normal brain (see above), they may be readily distinguished from hamartomas. Proton MR spectroscopy also helped us characterize an enhancing, but stable, mass in the cerebellum of a child with neurofibromatosis type 1 (57). Despite enhancement on MR images after gadolinium administration, this lesion showed proton MR spectra identical to that of normal cerebellum. In this patient, this information led to the avoidance of surgery, and the lesion has remained unchanged for 4 years after its discovery. In a different patient with neurofibromatosis type 1 and a cerebellar mass that demonstrated growth in a 12-month period, proton MR spectroscopy showed changes compatible with a tumor, and resection yielded a low-grade astrocytoma.

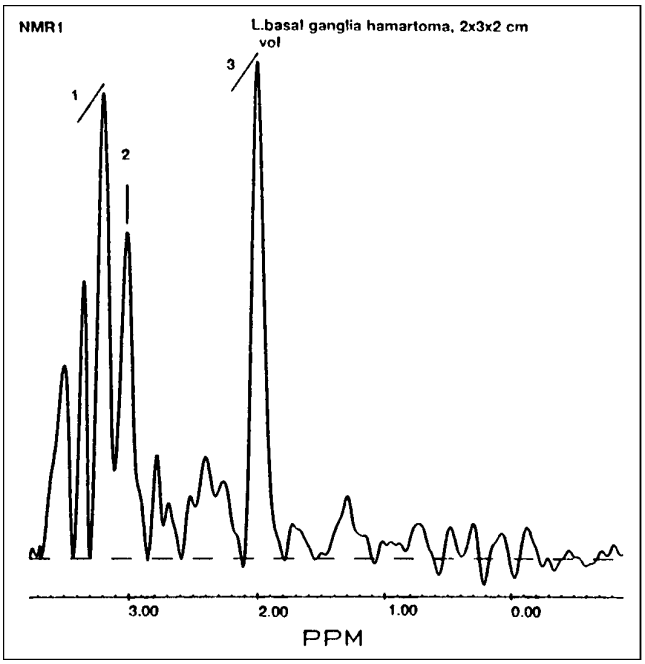

Fig 12. Hamartoma in neurofibromatosis type 1. Single-volume proton MR spectroscopy in left basal ganglia hamartoma in a patient with neurofibromatosis type 1 shows normal Cho (*1*) and Cr (*2*) and minimally decreased NAA (*3*). These findings are remarkably similar to normal brain (compare with Fig 1) and very different from those expected in glial malignancies (compare with Fig 4) (from Castillo et al [56]).

Cerebral Heterotopias

Small gray matter heterotopias are found in as many as 10% of children with medically refractory seizures (58). These are easily diagnosed by MR images, because they parallel the signal intensity of normal cortex in all sequences and do not enhance after contrast administration. Rarely, these heterotopias may be very large, and because they may contain cerebrospinal fluid spaces and vessels, they may be confused with tumors. Biopsies of such lesions will further confound the diagnosis, because the pathologist may interpret them as ganglion cell tumors (58). In these lesions, proton MR spectroscopy may show that their metabolite concentrations are identical or very

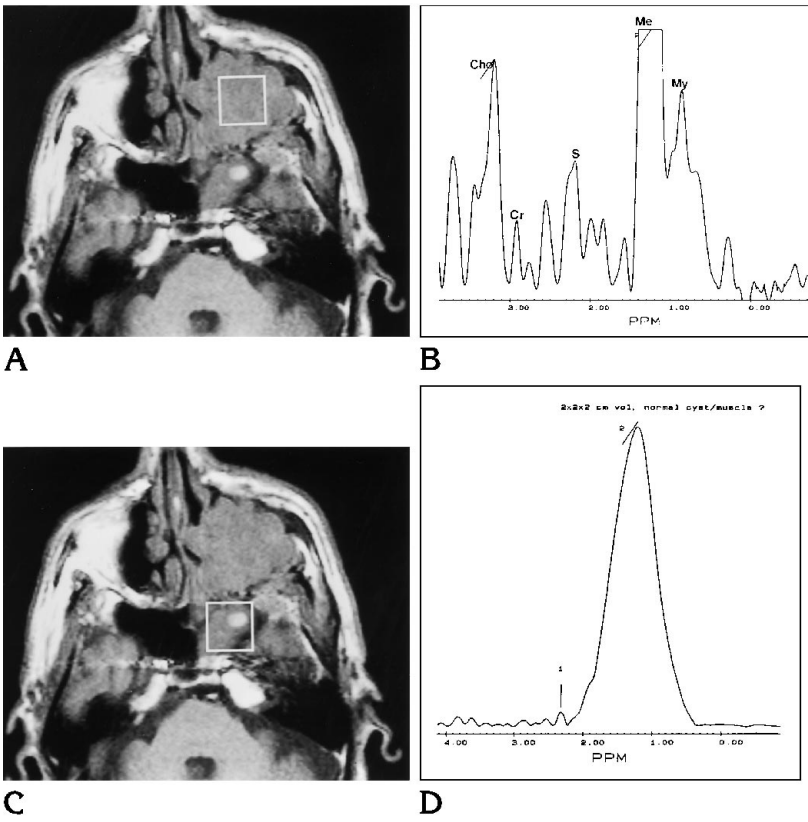

Fig 13. Maxillary sinus squamous cell carcinoma.

A, Axial MR T1-weighted image (600/15/2) shows the location of the voxel within the mass in the left maxillary sinus (proved squamous cell carcinoma).

B, Proton MR spectroscopy shows elevated Cho with respect to Cr. *S* indicates sialic acid, which is present in malignancies outside the central nervous system; *ME*, methylene; and *My*, methyl; both are found in membrane lipids of malignancies.

C, Axial MR T1-weighted image (600/15/2) shows the voxel encompassing the left-sided compartment of the sphenoid sinus. It was unclear whether the opacification of this sinus was secondary to postobstructive inflammation or tumor invasion.

D, Proton MR spectroscopy from the sphenoid sinus shows no discernible Cho or Cr. A small peak for sialic acid (*1*) is present. A large peak (*2*) at 1.3 ppm may be related to lipids in inflammatory tissues. At surgery, there were only inflammatory mucosa changes and retained secretions in this region.

similar to that of normal brain, thereby establishing the diagnosis of giant heterotopia (hamartomatous malformation) (17).

Multiple Sclerosis

MR images with contrast will show enhancement in active multiple sclerosis lesions. It has been shown that NAA is decreased in patients with chronic multiple sclerosis in whom axonal loss has occurred (59). Conversely, in acute plaques, NAA may be normal, indicating that the axons have not yet disappeared or have been permanently damaged. In addition, resonances corresponding to free lipids (0.9 to 1.6 ppm) have been observed in chronic multiple sclerosis plaques and may reflect disintegration of myelin.

Malignant Head and Neck Tumors

Proton MR spectroscopy has been used to study orbital tumors (60, 61). Despite their relatively small size, adequate MR spectra may be obtained in vivo. Ocular melanotic melanomas show a large peak at 6.72 ppm that corresponds to melanin (61). Preliminary data also indicate that proton MR spectroscopy may be used to characterize extracranial head and neck malignancies in vivo (61, 62). Lipomas show resonances at 1.29 and 2.13 ppm that correspond to lipids. Proton MR spectroscopy may also be useful in separating truly benign follicular thyroid masses from follicular malignancies (63). Thyroid carcinomas show resonances from amino acids, glutamate (2.20 ppm), and valine (0.71 ppm) (64).

At our institution we have found that an increased Cho/Cr ratio is present in all squamous cell carcinomas of the upper aerodigestive track when compared with normal tissues (Mukherji SK, Schiro S, Castillo M, Kwock L, Soper R, Blackstock W, unpublished data) (Fig 13). We have confirmed this preliminary observation by analyzing tissue blocks from squamous cell carcinomas with proton MR spectroscopy at 11 T. Currently, we are evaluating the potential utility of proton MR spectroscopy in the differentiation of recurrent and residual tumors from posttreatment changes, monitoring the response of tumors during and after treatment, attempting to detect and to characterize occult nodal metastases in sites that are indeterminate by both

physical examination and imaging studies, and detecting unknown primary sites.

References

1. Purcell EM, Torrey HC, Pound RV. Resonance absorption by nuclear magnetic moments in solids. *Physiol Rev* 1946;69:37–38
2. Bloch R, Hansen WW, Packard M. Nuclear induction. *Physiol Rev* 1946;69:127
3. Protor WG, Yu FC. The dependence of nuclear magnetic resonance frequency upon chemical shift. *Physiol Rev* 1950;70:717
4. Lenkinski RE, Schnall MD. MR spectroscopy and the biochemical basis of neurological disease. In: Atlas SW, ed. *Magnetic Resonance Imaging of the Brain and Spine*. New York: Raven, 1991: 1099–1121
5. Bottomley PA, Foster TB, Darrow RB. Depth-resolved surface coil spectroscopy (DRESS) for in-vivo H-1, P-31, and C-13 NMR. *J Magn Reson* 1984;59:338–342
6. Luyten PR, Marien AJH, Systma B, et al. Solvent suppressed spatially resolved spectroscopy: an approach to high resolution NMR on a whole body MR system. *J Magn Reson* 1989;9:126–131
7. Frahm J, Bruhn H, Gyngell ML, et al. Localized high resolution proton NMR spectroscopy using stimulated echoes: initial applications to human brain in vivo. *Magn Reson Med* 1989;9:79–93
8. Fulham MJ, Bizzi A, Dietz MJ, et al. Mapping of brain tumor metabolites with proton MR spectroscopic imaging: clinical relevance. *Radiology* 1992;185:675–686
9. van der Knaap MS, van der Grond J, van Rijen PC, et al. Age-dependent changes in localized proton and phosphorus MR spectroscopy of the brain. *Radiology* 1990;176:509–515
10. Miller BL. A review of chemical issues in 1H NMR spectroscopy: *N*-acetyl-L-aspartate, creatine, and choline. *NMR Biomed* 1991; 4:47–52
11. Kreis R, Ernst T, Ross BD. Development of the human brain: in vivo quantification of metabolite and water content with proton magnetic resonance spectroscopy. *Magn Reson Med* 1993;30: 424–437
12. Sanders JA. Magnetic resonance spectroscopy. In: Orrison WW, Lewine JD, Sanders JA, Harthshorne MF, eds. *Functional Brain Imaging*. St Louis: Mosby, 1995:419–467
13. van der Knaap MS, Ross B, Valk J. Uses of MR in inborn errors of metabolism. In: Kucharczyk J, Mosely M, Barkovich AJ, eds. *Magnetic Resonance Neuroimaging*. Boca Raton: CRC Press, 1994:245–318
14. Ceodan S, Parrilla R, Santoro J, Rico M. H-1 NMR detection of cerebral/myo-inositol. *FEBS Lett* 1985;187:167–172
15. Miller BL, Moats RA, Shonk T, et al. Alzheimer disease: depiction of increased cerebral myo-inositol with proton MR spectroscopy. *Radiology* 1993;187:433–437
16. Michealis T, Merboldt KD, Bruhn H, Dipl Math WH, Frahm J. Absolute concentrations of metabolites in the adult human brain in vivo: quantification of localized proton MR spectra. *Radiology* 1993;187:219–227
17. Castillo M, Kwock L, Scatliff JH, Gudeman S, Greenwood R. Proton MR spectroscopic characteristics of a presumed giant subcortical heterotopia. *AJNR Am J Neuroradiol* 1993;14:426–429
18. Luyten PR, Marien AJH, Heindel W, et al. Metabolic imaging of patients with intracranial tumors: H-1 MR spectroscopic imaging and PET. *Radiology* 1990;176:791–799
19. Bruhn H, Frahm J, Gyngell ML, et al. Noninvasive differentiation of tumors with use of localized H-1 MR spectroscopy in vivo: initial experience in patients with cerebral tumors. *Radiology* 1989;172: 541–548
20. Gill SS, Thomas DG, Van Bruggen N, et al. Proton MR spectroscopy of intracranial tumors: in vivo and in vitro studies. *J Comput Assist Tomogr* 1990;14:497–504
21. Kugel H, Heindel W, Ernestus RI, Bunke J, du Mesnil R, Friedmann G. Human brain tumors: spectral patterns detected with localized H-1 MR spectroscopy. *Radiology* 1992;183:701–709
22. Demaerel P, Johannik K, Van Hecke P, et al. Localized H-1 NMR spectroscopy in fifty cases of newly diagnosed intracranial tumors. *J Comput Assist Tomogr* 1991;15:67–76
23. Ott D, Hennig J, Ernst T. Human brain tumors: assessment with in vivo proton MR spectroscopy. *Radiology* 1993;186:745–752
24. Sijens PE, van Dijk P, Oudkerk M. Correlation between choline level and Gd-DTPA enhancement in patients with brain metastases of mammary carcinomas. *Magn Reson Med* 1994;32:549–555
25. Gober JR. Noninvasive tissue characterization of brain tumor and radiation therapy using magnetic resonance spectroscopy. *Neuroimaging Clin North Am* 1993;3:779–802
26. Barker PB, Lee RR, McArthur JC. AIDS dementia complex: evaluation with proton MR spectroscopic imaging. *Radiology* 1995; 195:58–64
27. Jarvik JG, Lenkinski RE, Grossman RI, Gomori JM, Schanll MD, Frank I. Proton MR spectroscopy of HIV-infected patients: characterization of abnormalities with imaging and clinical correlation. *Radiology* 1993;186:739–744
28. Chong WK, Sweeny B, Wilkinson ID, et al. Proton spectroscopy of the brain in HIV infection: correlation with clinical, immunologic, and MRI findings. *Radiology* 1993;188:119–124
29. Cortey A, Jarvik JG, Lenkinski RE, Grossman RI, Frank I, Delivoria-Papadopoulos M. Proton MR spectroscopy of brain abnormalities in neonates born to HIV-positive mothers. *AJNR Am J Neuroradiol* 1994;15:1853–1859
30. Shonk TK, Moats RA, Gifford P, et al. Probable Alzheimer disease: diagnosis with proton MR spectroscopy. *Radiology* 1995; 195:65–72
31. Miller BL, Moats RA, Shonk T, Ernst T, Woolley S, Ross BD. Alzheimer disease: depiction of increased cerebral *myo*-inositol with proton MR spectroscopy. *Radiology* 1993;187:433–437
32. Rango M, Spagnoli D, Tomei G, Bamont F, Scarlato G, Zetta L. Central nervous system Trans-synaptic effects of acute axonal injury: a H-1 magnetic resonance study. *Magn Reson Med* 1995; 33:595–600
33. Bowen BC, Block RE, Sanchez-Ramos J, et al. Proton MR spectroscopy of the brain in 14 patients with Parkinson disease. *AJNR Am J Neuroradiol* 1995;16:61–68
34. van der Knaap MS, van der Grond J, Luyten PR, den Hollander JA, Nauta AAP, Valk J. H-1 and P-31 magnetic resonance spectroscopy of the brain in degenerative cerebral disorders. *Ann Neurol* 1993;31:202–211
35. Grodd W, Krageloh-Mann I, Klose U, Sauter R. Metabolic and destructive brain disorders in children: findings with localized proton MR spectroscopy. *Radiology* 1991;181:173–181
36. Tzika AA, Ball WS, Vigneron DB, Dunn RS, Nelson SJ, Kirks DR. Childhood adrenoleukodystrophy: assessment with proton MR spectroscopy. *Radiology* 1993;189:467–480
37. Marks HG, Caro PA, Wang Z, et al. Use of computed tomography, magnetic resonance imaging, and localized 1H magnetic resonance spectroscopy in Canavan's disease: a case report. *Ann Neurol* 1991;30:106–110
38. Grodd W, Krageloh-Mann I, Petersen D, Trefz FK, Harzer K. In vivo assessment of *N*-acetylaspartate in brain in spongy degeneration (Canavan's disease) by proton spectroscopy. *Lancet* 1990;336: 437–438

39. Castillo M, Kwock L, Green C. MELAS syndrome: imaging and proton MR spectroscopic findings. *AJNR Am J Neuroradiol* 1995; 16:233–239
40. Barkovich AJ, Good WV, Koch TK, Berg BO. Mitochondrial disorders: analysis of their clinical and imaging characteristics. *AJNR Am J Neuroradiol* 1993;14:1119–1137
41. Kreis R, Ross BD, Farrow NA, Ackerman Z. Metabolic disorders of the brain in chronic hepatic encephalopathy detected with H-1 MR spectroscopy. *Radiology* 1992;182:19–27
42. Ross BD, Jacobson S, Villamil F, et al. Subclinical hepatic encephalopathy: proton MR spectroscopic abnormalities. *Radiology* 1994;193:457–463
43. Barker PB, Gillard JH, van Zijl PCM, et al. Acute stroke: evaluation with serial proton MR spectroscopic imaging. *Radiology* 1994; 192:723–732
44. Bruhn H, Frahm J, Gyngell ML, Merboldt KD, Hanick W, Sauter R. Cerebral metabolism in man after acute stroke: new observations using localized proton MR spectroscopy. *Magn Reson Med* 1989; 9:126–131
45. Duijn JH, Matson GB, Maudsley AA, Hugg JW, Weiner MW. Human brain infarction: proton MR spectroscopy. *Radiology* 1992; 183:711–718
46. Behar KL, den Hollander JA, Stromski ME, et al. High-resolution H-1 nuclear magnetic resonance study of cerebral hypoxia in vivo. *Proc Natl Acad Sci USA* 1983;80:4945–4948
47. Marshall VG, Bradley WG, Marshall CE, Bhoopat T, Rhodes RH. Deep white matter infarction: correlation of MR imaging and histopathologic findings. *Radiology* 1988;167:517–522
48. Sappey-Marinier D, Calabrese G, Hetherington HP, et al. Proton magnetic resonance spectroscopy of human brain: applications to normal white matter, chronic infarction, and MRI white matter signal hyperintensities. *Magn Reson Med* 1992;26:313–327
49. Sibbitt WL, Haseler LJ, Griffey RH, Hart BL, Sibbitt RR, Matwiyoff NA. Analysis of cerebral structural changes in systemic lupus erythematosus by proton MR spectroscopy. *AJNR Am J Neuroradiol* 1994;15:923–928
50. Kuzniecky RI, Jackson GD. *Magnetic Resonance in Epilepsy*. New York: Raven, 1995:289–314
51. Ng TC, Comair YG, Xue M, et al. Temporal lobe epilepsy: presurgical localization with proton chemical shift imaging. *Radiology* 1994;193:465–472
52. Kuzniecky RI, Jackson GD. *Magnetic Resonance in Epilepsy*. New York: Raven, 1995:213–324
53. Komoroski RA. Measurement of psychoactive drugs in the human brain in vivo by MR spectroscopy. *AJNR Am J Neuroradiol* 1993; 14:1038–1042
54. Gonzalez RG, Guimaraes AR, Sachs GS, Rosembaum JF, Garwood M, Renshaw PF. Measurement of human brain lithium in vivo by MR spectroscopy. *AJNR Am J Neuroradiol* 1993;14: 1027–1037
55. Sevick RJ, Barkovich AJ, Edwards MSB, et al. Evolution of white matter lesions in neurofibromatosis type 1: MR findings. *AJR Am J Roentgenol* 1992;159:171–175
56. Castillo M, Green C, Kwock L, et al. Proton magnetic resonance spectroscopy in patients with NF-1: evaluation of hamartomas and clinical correlation. *AJNR Am J Neuroradiol* 1995;16:141–147
57. Castillo M, Kwock L, Green C, Schiro S, Wilson JD, Greenwood R. Proton MR spectroscopy in a possible enhancing hamartoma in a patient with neurofibromatosis type 1. *AJNR Am J Neuroradiol* 1995;16:993–996
58. Barkovich AJ, Kjos BO. Gray matter heterotopias: MR characteristics and correlation with developmental and neurologic manifestations. *Radiology* 1992;182:493–499
59. Arnold DL, Matthews PM, Francis G, Antel J. Proton magnetic resonance spectroscopy of human brain in vivo in the evaluation of multiple sclerosis: assessment of the load of disease. *Magn Reson Med* 1990;14:154–159
60. Gomori JM, Grossman RI, Shields JA, Augsburger JJ, Joseph PM, DeSimeone D. Ocular MR imaging and spectroscopy: an ex vivo study. *Radiology* 1986;160:201–205
61. Mafee MF, Barany M, Gotsis ED, et al. Potential use of in vivo proton spectroscopy for head and neck lesions. *Radiol Clin North Am* 1989;27:243–254
62. McKenna WG, Lenkinski RE, Hendrix RA, Vogele KE, Bloch P. The use of magnetic resonance imaging and spectroscopy in the assessment of patients with head and neck and other superficial human malignancies. *Cancer* 1989;64:2069–2075
63. Johnson M, Selinsky B, Davis M, et al. In vitro NMR evaluation of human thyroid lesions. *Invest Radiol* 1989;24:666–671
64. Russell P, Lean CL, Delbridge L, May GL, Dowd S, Mountformd CE. Proton magnetic resonance and human thyroid neoplasia, I: discrimination between benign and malignant neoplasms. *Am J Med* 1994;96:383–388